American Journal of Materials Science 2014, 4(4): 169-177
DOI: 10.5923/j.materials.20140404.03

Hybrids of Polystyrene-b-Poly(ethylene-ran-butylene)-b-Polystyrene Reinforced by Electrospun Polyimide/ Carbon Nanotube Nanofibers: Preparation and Properties

Ayesha Kausar

Nanosciences and Catalysis Division, National Centre For Physics, Quaid-i-Azam University Campus, Islamabad, Pakistan

Abstract Using electrospinning technique, well-aligned poly(azo-ether-imide) (PAEI) nano-fibers and PAEI/multi-walled carbon nanotube (MWCNT) nano-fibers were developed in this effort. Afterwards, polystyrene-*b*-poly (ethylene-*ran*-butylene)-*b*-polystyrene (SEBS) and polyimide-based nano-fiber films were casted. The as-prepared electrospun nanofibers acted as homogeneous reinforcement to enhance the tensile strength and heat resistance of the films. Compared with neat SEBS, tensile strength of the films reinforced with PAEI and PAEI/MWCNT nano-fibers remarkably increased by >181%. The significant enhancement in the overall mechanical properties of the PAEI/MWCNT nano-fibers reinforced SEBS films was credited to fine compatibility between the electrospun nano-fibers and the matrix as well as superior nano-fiber orientation in the matrix. The homogeneous alignment of PAEI/MWCNT nano-fibers was also studied using SEM micrographs. Moreover, the thermal stability of PAEI/MWCNT nano-fibers reinforced SEBS found to be superior having 10% gravimetric loss in the range 591-602℃ and glass transition temperature of 238-255℃ relative to the neat polymer and PAEI nano-fiber-based system.

Keywords Polyimides, Electrospun nanofibers, Thermostability, Elastomers, Mechanical properties

1. Introduction

Polymer nanocomposites have gained immense significance, in recent years owing to several scientific and economical benefits. The inclusion of nanometer-scale reinforcement such as layered silicates, nanofiber, nanotubes, and nanoparticles in polymeric materials may dramatically improve the preferred properties of the related polymer [1]. These nanocomposites demonstrate superior physical properties such as enhanced mechanical strength, superior heat retardancy, improved flame retardancy, etc. Multi-walled carbon nanotubes (MWCNTs) are generally used as filler in polymer nanocomposites due to their attractive chemical intercalation nature [2, 3]. Addition of nanotubes to polymer/MWCNTs hybrids results in the great enhancement in mechanical, thermal and optical behaviors. Generally, the factors that limit the potential relevance of polymer nanocomposites are the compatibility between organic polymer and nanotubes, the extent of exfoliation in polymer matrix, and ductility/toughness of the polymer nanocomposites. Recently, enormous research efforts have contributed to improve the compatibility, dispersion and toughness of the polymer nanocomposites [4, 5]. In a typical immiscible polyblending system, a satisfactory physicomechanical behavior critically depends on the proper interfacial tension to engender small phase size and strong interfacial adhesion to transmit load between two phases. According to several literature reports, the block or graft copolymer may offer lowering of interfacial energy, and improvement of the interfacial adhesion between two phases [6–10]. Consequently, multiphase polymer systems form a significant area of polymer science, and the enhancement of physical properties of blends depends to a large extent on the degree of dispersion. Various thermoplastic elastomers such as polystyrene-*b*-polybutadiene-*b*-polystyrene (SBS), polystyrene-*b*-polyisoprene-*b*-polystyrene (SIS), and hydrogenated triblock copolymers have been developed and widely used [11]. The elastomers demonstrate fine process-ability under the melting conditions and the elasticity under the service conditions, which are typical for the thermoplastics and the vulcanized rubbers, respectively. The service conditions of conventional thermoplastic are often restricted by the glass transition temperature (T_g) of polystyrene blocks (100°C), since the hard polystyrene end blocks act as a cross-linker under the T_g by forming the

* Corresponding author:
asheesgreat@yahoo.com (Ayesha Kausar)
Published online at http://journal.sapub.org/materials
Copyright © 2014 Scientific & Academic Publishing. All Rights Reserved

spheric or cylindrical microdomains separated in the continuous polydiene phase. The incorporation of bulky and rigid alicyclic substituents is particularly effective to increase the T_g's of parent polymers [12-14]. The analysis of flow behavior is important and helpful for correlating the structure, morphology and rheological properties of polymer blends. High-performance polyimide blends are of considerable interest in this regard. Polyimide is predominantly attractive for their excellent heat stability and mechanical properties and frequently used as high-performance engineering plastics [15-19]. Polyimides own fine process-ability as well as chemical resistance. The combination of MWCNT and polyimide may provide mutually complementary properties; however, their immiscibility requires a proper compatibility. Therefore, various compatibilizers have been developed to control the phase structure of these blends. A well known, low-cost and effective method is the production of polymeric nano-fibers *via* electrospinning [20–22]. Electrospinning is recognized as an efficient technique for the fabrication of polymer nanofibers. Potential applications based on such fibers specifically their use as reinforcement in nanocomposite development has been realized. Accordingly, the electrospun nano-fibers are known as ideal candidates for reinforcing polymer materials due to extraordinary properties for instance excellent mechanical strength, high aspect ratio and surface-to-volume ratios [23]. In the current effort, we have fabricated polystyrene-*b*-poly(ethylene-*ran*-butylene)-*b*-polystyrene (SEBS) elastomer and polyimide-based nanofiber films. Initially, well-aligned homogeneous poly(azo-ether-imide) (PAEI) nano-fibers and PAEI/multi-walled carbon nanotube (MWCNT) nano-fibers were produced as reinforcing filler. Fine compatibility between the electrospun nano-fibers and the matrix was attained simply with out the chemical modification of the polyimide nano-fibers or addition of any coupling agent. Newly developed aligned poly(azo- ether-imide) fibers are efficient load transferring materials from the matrix to nano-fibers. As a consequence, the mechanical properties of films outstandingly improved by incorporating the PAEI and PAEI/MWCNT nano-fibers. Quite interestingly, the electrospun nano-fibers not only improved the tensile strength but also the tensile strain at break of the films. The as-prepared high-performance nanocomposite films also showed enhanced thermal properties after the incorporation of nano-fibers relative to pristine polyimide and SEBS. New polyimide films may act as potential contenders for light-weight aerospace materials.

2. Experimental

2.1. Materials

Polystyrene-*b*-poly(ethylene-*ran*-butylene)-*b*-polystyrene (SEBS) elastomer with molecular weight 118,000 (28% styrene content) supplied by Aldrich (St. Louis, Missouri, USA) was used in the synthesis of hybrid materials. MWCNT were prepared by our patented technology [24]. 4,4'-Oxydianniline (ODA) (97%), pyromellitic dianhydride (PMDA) (97%), 1,4-phenylenediamine (PDA) (97%) and N,N-dimethylacetamide (DMAc) (99%) were obtained from Aldrich. Ammonium thiocyanate (98%) and tetrahydrofuran (THF, 99.5%) were supplied by Fluka (Biocen GmbH, Duesseldorf, Germany). Dimethyl sulfoxide (DMSO) (99%) was procured from Merck, Nottingham, UK.

2.2. Measurements

NMR spectra were scanned at room temperature using BRUKER (Tokyo, Japan) Spectrometer (300.13 MHz for ^{1}H NMR) in deutrated DMSO. IR spectra were recorded using FTIR Spectrometer, Model No. FTSW 300 MX, manufactured by BIO-RAD, California, USA (4 cm^{-1} resolution). The number and weight-average molecular weight (M_n & M_w) was calculated through gel-permeation chromatography (GPC) and refractive index (RI) detector. Field Emission Scanning Electron Microscopy (FE-SEM) of freeze fractured samples was performed using JSM5910, JEOL Japan. Thermal stability was verified by METTLER TOLEDO TGA/SDTA 851 thermo gravimetric analyzer (California, USA) using 1–5 mg of the sample in Al_2O_3 crucible at a heating rate of 10 ℃/min. The dynamic mechanical thermal analysis was performed on hybrid materials in the temperature range of 0–300℃ with DMTA Q800 (frequency of 5 Hz, heated at 10 °C/min). Stress-strain response of the samples was obtained on Universal Testing Machine INSTRON 4206 (Norwood, United States) according to the ASTM 638 method. A crosshead speed of 100 mm/min was used during the test. To determine various mechanical properties, standard procedures and formulae were used. Three concurrent readings for each composite membrane were obtained and then the values were reported after taking the mean.

2.3. Synthesis of 1,4-phenylene bis(thiourea)

1,4-Phenylenediamine (0.4 mol), 30 mL of conc. HCl, ammonium thiocyanate (0.8 mol) and 200 mL of deaerated water were thoroughly mixed and heated in a porcelain dish for 2 h (on a steam bath) and allowed to cool to room temperature. The above mixture was evaporated to dryness for 6–7 h. Afterward the product obtained was boiled with charcoal (ethanol), filtered and cooled. 1,4-Phenylene bis(thiourea) was finally recrystallized from ethanol and dried under reduced pressure at 80℃ for 24 h [25].

2.4. Diazotization

4,4'-Oxydianniline (0.04 mol) was first added to conc. hydrochloric acid (10 mL) and then dissolved in distilled water (50 mL). The mixture was placed in ice-bath to cool to -10℃. To the above suspension, 0.04 mol sodium nitrite solution (20 mL) was added with continuous stirring. After the complete addition, mixture was allowed to stir for 1 h at -10℃ to avoid the decomposition of diazonium salt. The

excess of nitrite was removed by the addition of urea (2 g) with stirring of 0.5 h forming diazonium salt solution.

2.5. Synthesis of poly(azo-ether-imide)

The synthesis of poly(azo-ether-imide) was carried out in a 250 mL round bottom flask charged with 0.01 mol 1,4-phenylene bis(thiourea) and 50 mL DMAc. The mixture was stirred at 0 ℃ for 0.5 h. 0.01 mol pyromellitic dianhydride and diazonium salt solution was added and the mixture was again stirred at 0℃ for 1 h. Afterward, the mixture was stirred at room temperature for 24 h. The poly(amic acid) was precipitated by pouring the flask content into 200 mL water and methanol mixture. Then it was filtered, washed with hot water and dried overnight under vacuum dried at 70℃. A 250 mL two-necked round bottom flask equipped with a magnetic stirrer, nitrogen gas inlet tube was charged with 1.0 g of poly(amic acid) and 5 mL of dry DMAc and stirred. The mixture was stirred and afterward 5 mL acetic anhydride and 2.5 mL pyridine were added. The mixture was further stirred for 0.5 h and heated to 80℃ for 6 h [26]. The mixture was cooled and poured into water. Finally, it was filtered, washed with hot water and methanol and also dried under vacuum at 90℃ (Scheme 1). Spectral data substantiated the structure of the synthesized polymers FTIR and ^{1}H NMR analysis of the polymer is given in Table 1 and Fig. 1.

2.6. Solution Preparation

The precursor of polyimide, poly(amic acid) of poly(azo-ether-imide) (PAEI-PAA), was synthesized as described above. The polycondensation was performed in DMAc at 0 ℃, and the solid content of the pristine PAEI-PAA solution was 25 wt. %. For the preparation of neat PAEI-PAA solution used for electrospinning, it was diluted with DMAc; and for MWCNT (5 wt. %)/PAEI-PAA solution, the pristine PAEI-PAA solution was diluted by MWCNT(5 wt. %)//DMAc solution.

Prior to solution mixing, the MWCNT/DMAc solution was sonicated for 2 h to disperse the carbon nanotube homogeneously. Acetic anhydride and pyridine (2:1) was also added to the solutions.

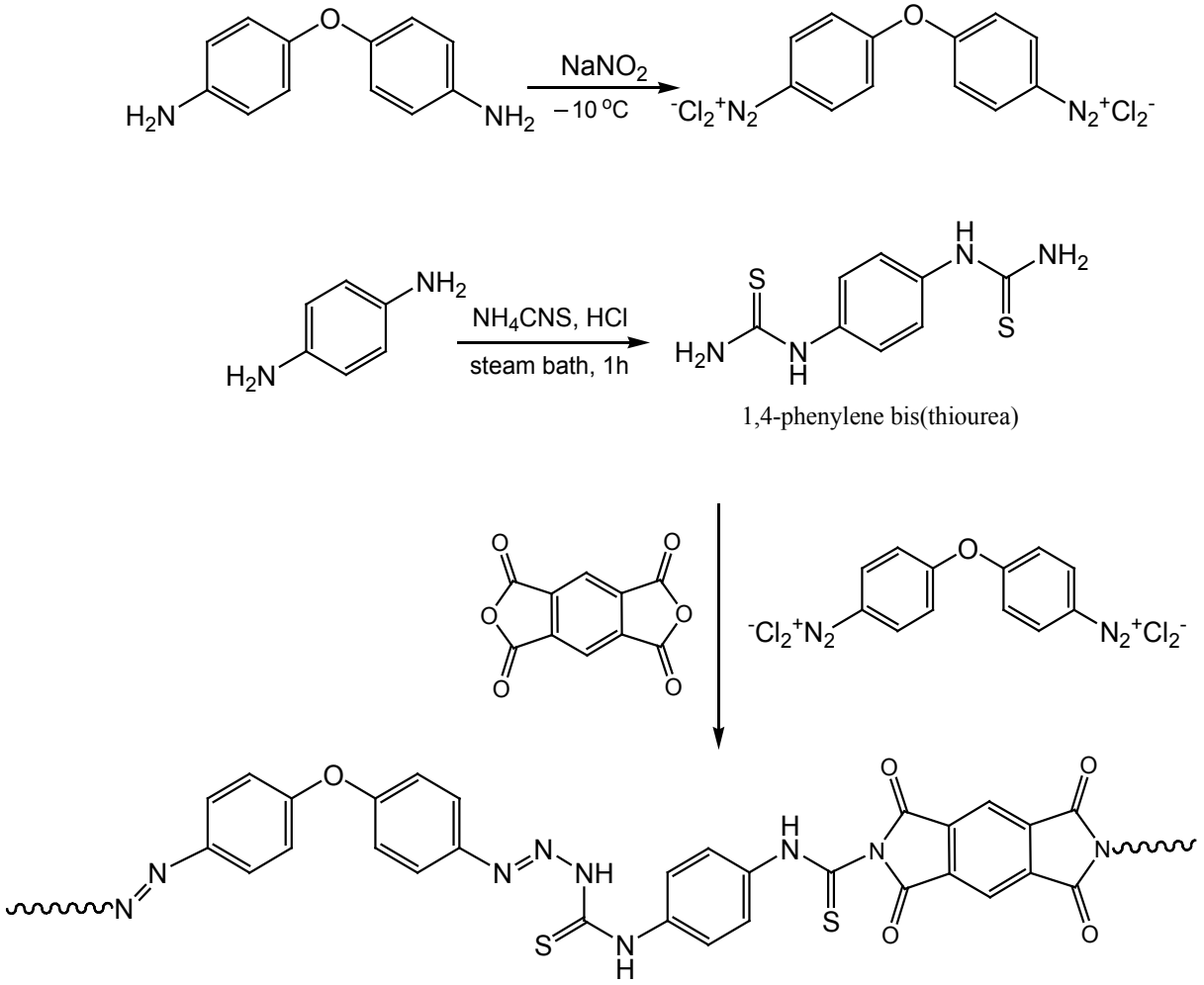

Scheme 1. Preparation of poly(azo-ether-imide)

Table 1. Structural analysis data of neat polymer, SEBS/PAEI and SEBS/PAEI/MWCNT nano-fiber film

Compound	FTIR		NMR
	Type of vibration	Frequency cm^{-1}	^1H NMR δ ppm
PAEI	N–H stretch	3233	9.28 (s) Sec. amine
	Aromatic C–H stretch	3009	8.99 (s) Anhydride ring protons
	Sym Imide C=O	1791	6.81-7.11 (d) ODA aromatic protons
	Asym Imide C=O	1721	6.21-6.45 (d) Phenylene protons
	N–H bend	1594	
	–N=N–	1412	
	C–O	1273	
	C=S	1123	
SEBS/PAEI 1	N–H stretch	3288	
	Aromatic C–H stretch	3005	
	Aliphatic C–H stretch	2912, 2856	
	Sym Imide C=O	1796	
	Asym Imide C=O	1723	
	N–H bend	1598	
	–N=N–	1414	
	C–O	1272	
	C=S	1123	
SEBS/PAEI/ MWCNT 1	N–H stretch	3311	
	Aromatic C–H stretch	3008	
	Aliphatic C–H stretch	2944, 2832	
	Sym Imide C=O	1789	
	Asym Imide C=O	1721	
	N–H bend	1596	
	–N=N–	1414	
	C–O	1276	
	C=S	1125	

2.7. Fabrication of nano-fibers

Electrospinning was carried out using a syringe with a spinneret (diameter 0.5 mm) and 25 kV applied voltage at 30 ℃ . The feeding rate was 0.25 mL/h and the spinneret-collector distance was set to be 10 cm. Neat PAEI and PAEI/MWCNT-based nano-fibers were collected using a rotating disk collector (diameter 0.30 m; width 10 mm). During electrospinning, the linear speed of rotating collector was about 10 ms^{-1}. All the electrospun nano-fibers were dried at 80℃ for 4 h to remove the residual solvent followed by an annealing at each temperature stage for 1 h.

2.8. Preparation of Nano-fibers Reinforced Films

The desired amount of as-prepared electrospun (neat PAEI and PAEI/MWCNT) nano-fibers were immersed in the solution of SEBS (1 g in 10 mL DMAc) for 1 h and heated to 80ºC to obtain the nano-fiber reinforced nanocomposite films. Table 1 depicts the structural data of SBS/PAEI and SBS/PAEI/MWCNT nano-fibers reinforced nanocomposites.

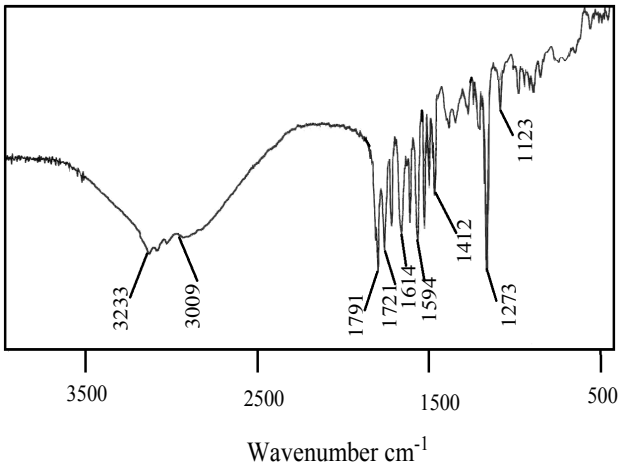

Figure 1. FTIR spectrum of neat PAEI

3. Results and Discussion

3.1. Mechanical Properties

Typical stress-strain curves of neat cast PAEI film and well-aligned nano-fiber reinforced films are given in Fig. 2. Table 2 lists the tensile properties including tensile strength, tensile modulus and elongation at break. Tensile strength of electrospun PAEI/MWCNT nano-fiber reinforced films i.e. SEBS/PAEI/MWCNT 1-3 was much higher relative to SEBS/PAEI 1-3 containing PAEI nano-fiber, owing to fine orientation of the former electrospun nano-fibers in the films. Tensile strength of neat PAEI was 182.3 MPa which increased to 223.0 MPa with 1 wt. % PAEI/MWCNT loading. The property further increased with the loading of 2 and 3 wt % filler as 233.7 and 249.6 MPa respectively. On the other hand, increasing PAEI nano-fiber content from 1 to 3 wt. % increased the tensile strength from 188.2 to 199.1 MPa. Seeing that, incorporation of 3 wt. % highly aligned PAEI/MWCNT nano-fibers as reinforcing agent, caused the tensile strength to increase about 20% (SEBS/PAEI/ MWCNT 3) relative to SBS/PAEI 3 film. Tensile modulus of SEBS/PAEI/MWCNT 1-3 increased from 11.1 to 14.5 GPa. This was considerably higher than those of 1-3 wt. % PAEI nano-fiber reinforced films because of better compatibility between PAEI/MWCNT fibers and the matrix. It is well known that the mechanical properties of nanofiller-filled

polymer matrix, especially the strength and modulus depend to a great extent on filler dispersion and interfacial interaction [26, 27]. Fig. 2 shows that the tensile strength increased with the raise of weight percentage of nanofiller. The tensile strength of all composite specimens give better strength compared to neat PAEI and SEBS. The tensile strength of PAEI increased about 8.5% in SEBS/PAEI 3, while 27% in SEBS/PAEI/MWCNTs 3. Compared with SEBS matrix, the tensile strength improved about 97% in SEBS/PAEI 3, while 98% in SEBS/PAEI/MWCNTs 3. These results clearly indicated that the nano-fibers improved the tensile strength of neat resins. Nevertheless, the proper dispersion of nano-fibers has great affect on the mechanical properties. With the increase of filler ratio, the tensile strength was enhanced, probably due to the alignment of the two different nano-fibers not forming large particles that could be uniformly distributed within the matrix.

The elongation at break for the SEBS/PAEI/ MWCNT-based nano-fiber films also improved from 31.1 to 34.8% by incorporating 1-3 wt. % PAEI/MWCNT nano-fibers. On the contrary, the elongation at break for the PAEI films improved 27.6 to 30.8% by incorporating 1-3 wt. % PAEI nano-fibers. The significant improvement of tensile properties of the PAEI/MWCNT nano-fiber reinforced SEBS film can be ascribed to dual orientation *(i)* well-oriented electrospun PAEI nano-fibers and *(ii)* well-oriented nanotubes in the electrospun PAEI nano-fibers. The PAEI nano-fiber reinforced SEBS films were transparent; however the PAEI/MWCNT-based films were blackish in color. The significant improvement in overall mechanical properties of SEBS/PAEI/MWCNT films was attributed to the fine compatibility and strong interfacial interaction between nano-fibers and matrix. High-performance homogeneity reinforced SEBS/PAEI/ MWCNT 1-3 nanocomposites were successfully prepared with high toughness (4974-5743 MPa) and overall enhanced mechanical properties by incorporation of 1-3 wt. % nano-fibers as reinforcing agents. Here, again the toughness of SEBS/PAEI 1-3 nanocomposites was relatively low (3344-5122 MPa). In other words, compared with the 3 wt. % PAEI nano-fiber reinforced film, the tensile strength for film reinforced with 3 wt. % PAEI/MWCNT nano-fibers significantly increased by 11%. The mechanical properties appear to be significantly superior to reported electrospun fiber-based composites [28-30].

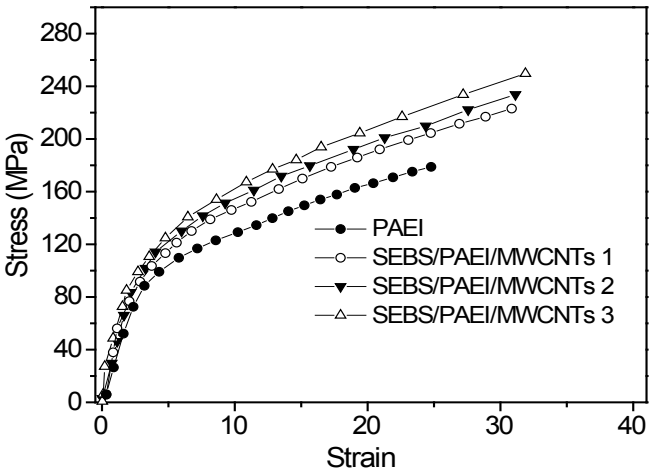

Figure 2. Stress-strain curves of PAEI and SEBS/PAEI/MWCNTs

3.2. Morphology

By electrospinning of PAEI/MWCNT-PAA solution and subsequent imidization, PAEI nano-fibers with MWCNT were prepared. Generally, the orientation and diameter uniformity of the electrospun nanofibers are of prime importance for attaining high strength and toughness.

Table 2. Mechanical properties of PAEI and SEBS/PAEI/MWCNTs

Composition	Tensile Stress (MPa) ± 0.1	Elongation at break ± 0.03	Tensile Modulus (GPa) ± 0.1	1Toughness (MPa) ± 0.2
PAEI	182.3	25.1	10.7	3291
[2]SEBS/PAEI/MWCNTs 1	223.0	31.1	11.1	4974
SEBS/PAEI/MWCNTs 2	233.7	33.3	13.2	5250
SEBS/PAEI/MWCNTs 3	249.6	34.8	14.5	5743
SEBS/PAEI 1	188.2	27.6	8.9	3344
SEBS/PAEI 2	192.7	28.9	9.4	4152
SEBS/PAEI 3	199.1	30.8	12.3	5122
SEBS	4.54	5.47	0.0043	21

[1]Toughness was determined by integrating the area under the stress-strain curve.
[2]The number in the sample designation refers to wt. % of nano-fibers in the sample.

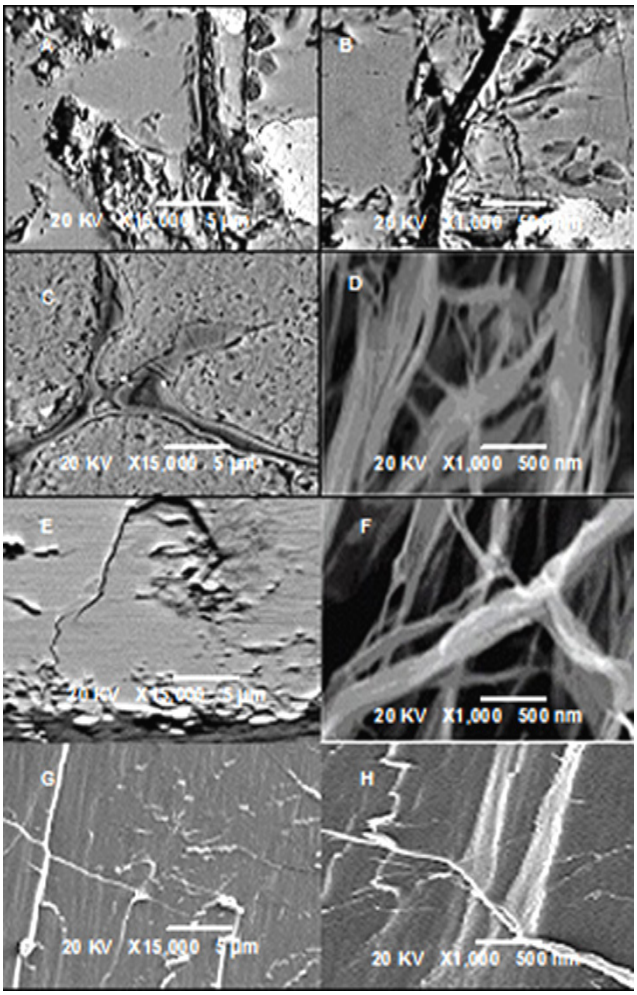

Figure 3. FESEM images of (A) SEBS/PAEI 1 at 5 µm; (B) SEBS/PAEI 1 at 500 nm; (C) SEBS/PAEI 3 at 5 µm; (D) SEBS/PAEI 3 at 500 nm; (E) SEBS/PAEI/MWCNTs 1 at 5 µm; (F) SEBS/PAEI/MWCNTs 1 at 500 nm; (G) SEBS/PAEI/MWCNTs 3 at 5 µm;; (H) SEBS/PAEI/MWCNTs 3 at 500 nm

Fig. 3 A & B show the micrographs of SEBS/PAEI 1 at 5 µm and 500 nm respectively. It can be seen that the nano-fibers were randomly dispersed in nanocomposite containing 1 wt. % PAEI filler. The reason is the absence of the carbon nanotubes, which were responsible for better alignment and orientation of the fabricated nano-filler. Fig. 3 C & D display the micrographs of SEBS/PAEI 3 at various resolutions. Relatively homogeneous distribution of PAEI/MWCNT nano-fibers was observed in the elastomer. Additionally with the increase in filler content, more fibers seemed to be coated heavily with the matrix. Fig. 3 E & F depict the micrographs of SEBS/PAEI/MWCNTs 1 at 5 µm and 500 nm respectively. Inclusion of nanotubes in the fibers renders them well-oriented without any agglomeration. The distribution was quite fine as compared to the morphology of SEBS/PAEI-based materials. The incorporation of greater wt. % of PAEI nano-fibers led to the more dense distribution; however the dispersion still remained uniform. Fig. 3 G & H reveal the morphology of SEBS/PAEI/MWCNTs 3 at various resolutions. Owing to high specific surface area, the composite fibers proffer sufficient shared boundary across two components for the polymer/filler interaction. Thus the polymer segments aligned with the adjoining filber particles formed well-oriented structure. As a result, these particulars turned out to be higher strength and modulus of the sample as shown in the tensile results presented in preceding section. Consequently, apposite interactions among carbon nano-fibers and matrix are essential to augment the physical proficiency of these materials. The fine dispersion and orientation of PAEI/MWCNTs fibers in SEBS favorably impacted the composite performance including mechanical and thermal profile.

3.3. Thermal Properties

Table 3. Thermal analyses data of PAEI and SEBS/PAEI/MWCNTs

Polymer	T_g (°C)	T_0 (°C)	T_{10} (°C)	T_{max} (°C)	Y_c at 650 °C (%)
PAEI	233	548	576	613	39
SEBS/PAEI/MWCNTs 1	238	551	591	646	44
SEBS/PAEI/MWCNTs 2	243	557	595	663	46
SEBS/PAEI/MWCNTs 3	255	559	602	674	53
SEBS/PAEI 1	120	522	579	609	40
SEBS/PAEI 2	129	531	588	624	42
SEBS/PAEI 3	137	539	593	633	45
SEBS	45,83	242	259	447	23

T_g : Glass transition temperature
T_0 : Initial decomposition temperature
T_{10} : Temperature for 10 % weight loss
T_{max} : Maximum decomposition temperature
Y_c : Char yield; weight of polymer remained

TGA thermograms for neat PAEI and different nano-fibers reinforced SEBS films are shown in Fig. 4. It is obvious from Table 3 that all the SEBS films reinforced by PAEI/MWCNT electrospun nano-fibers exhibited excellent thermal stability. In the case of neat PAEI, the initial degradation temperature T_0 was 548℃, 10% weight loss temperature was T_{10} 576℃, and T_{max} of 613℃ were experiential. Upon the addition of 1 wt. % PAEI/MWCNTs nano-fibers T_0 was raised to 551℃, T_{10} to 591℃, and T_{max} 646℃. The film with 2 wt. % PAEI/MWCNTs resulted in the T_0 557℃, T_{10} 595℃ and T_{max} 663℃. Consequently, 2 wt. % PAEI/MWCNTs nanocomposite showed higher thermal stability among the materials prepared (T_0 559℃, T_{10} 602℃ and T_{max} 674℃.). Thermal stability appeared to be relatively lower for PAEI nano-fiber-based system. SEBS/PAEI 1 (1 wt. % nanofiber) showed T_0 522℃; T_{10} 579℃; and T_{max} 609℃, while SEBS/PAEI 3 (3 wt. % filler) revealed T_0 539℃; T_{10} 593℃; and T_{max} 633℃. Additionally, the char yield of the SEBS/PAEI/MWCNTs nano-hybrids sufficiently advanced from 44 to 53 % at 650℃. Quite the opposite, the char yield of PAEI nano-fibers hybrids had lower values of 40-45%. Dynamic mechanical analysis was used to study the glass transition (T_g) of the nanocomposite films from loss tangent of DMA. As shown in Fig. 5, loss tangent (tan δ) of the SEBS/PAEI/MWCNTs showed increase in segmental T_g. With increasing wt. % of

PAEI/MWCNT nano-fiber in system, the glass-transition temperature was shifted from 233 (neat PAEI) to 255℃ (3 wt. % PAEI/MWCNTs nano-fibers). The improved glass transition indicated better segmental rigidity owing to the restriction of chains bonded to carbon nanotubes.

In the case of SEBS/PAEI system, the increase in glass transition occurred from 120 to 137℃, but it was much lower than that of SEBS/PAEI/MWCNTs system. The SEBS/PAEI film containing 3 wt. % PAEI nano-fibers possessed lower tan δ and glass transition temperature of 137℃ compared with neat PAEI but much higher than SEBS elastomer. Consequently, the SEBS film with PAEI nano-fibers had higher T_g than the neat block copolymer itself. Concisely, the homogeneity reinforcing method proved very successful for fabricating high mechanical performance SEBS//PAEI/MWCNTs nanocomposites. The homogeneity reinforcing method was very successful for fabricating high performance elastomer/polyimide nanocomposites compared with the reported ones [31].

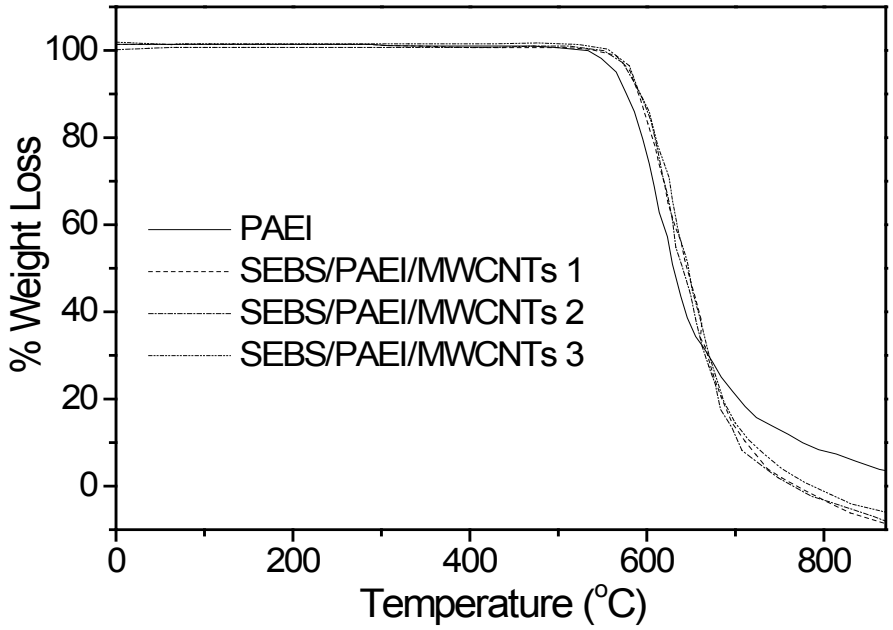

Figure 4. TGA curves of PAEI and SEBS/PAEI/MWCNTs at a heating rate 10 °C/min in N_2

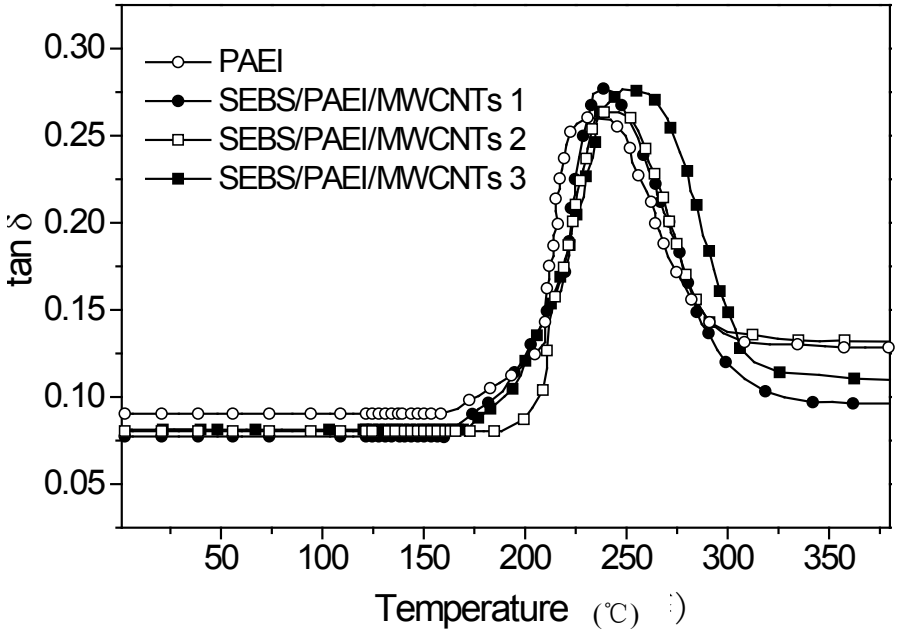

Figure 5. Variation of loss tangent (tanδ) with temperature for PAEI and SEBS/PAEI/MWCNTs films

4. Conclusions

High performance polystyrene-*b*-poly(ethylene -*ran*-butylene)-*b*-polystyrene elastomer-based hybrids reinforced with electrospun well-aligned PAEI and PAEI/MWCNTs nano-fibers were prepared in this endeavor. FESEM micrographs indicated that the SEBS/PAEI/MWCNTs had homogeneously dispersed and well oriented nano-fibers. According to results, the as-prepared PAEI/MWCNTs aligned electrospun nano-fibers may act as ideal reinforcing agents to fabricate high-performance nanocomposite films because of good compatibility between the electrospun nano-fibers and the matrix. The tensile strength, tensile modulus, elongation at break and toughness of SEBS/PAEI/ MWCNTs nanocomposite appeared to be superior compared with PAEI nano-fibers reinforced films. Likewise, SEBS/PAEI/MWCNTs nano-fiber films exhibited fine heat stability relative to neat PAEI and other nanohybrids. Novel approach to fabricate elastomer-based PAEI/MWCNTs nano-hybrid films utilizing electospun nano-fibers may be valuable for defense and aerospace purpose.

REFERENCES

[1] Coleman, J. N., Khan, U., Gunko, Y. K., 2006, Mechanical reinforcement of polymers using carbon nanotubes. Adv. Mater., 18(6), 689-706.

[2] Camponeschi, E., Vance, R., Al-Haik, M., Garmestani, H., Tannenbaum, R., 2007, Properties of carbon nanotube-polymer composites aligned in a magnetic field. Carbon 45(10), 2037-2046.

[3] Hill, D., Lin, Y., Qu, L. W., Kitaygorodskiy, A., Connell, J. W., Allard, L. F., Ya-Ping Sun, Y. –P., 2005, Functionalization of carbon nanotubes with derivatized polyimide. Macromolecules, 38(18), 7670-7675.

[4] Strobl, C. J., Schaflein, C., Beierlein, U., Ebbecke, J., Wixforth, A., 2004, Carbon nanotube alignment by surface acoustic waves. Appl. Phys. Lett., 85(8), 1427-1429.

[5] Baji, A., Mai, Y. W., Wong, S. C., Abtahi, M., Du, X. S., 2010, Mechanical behavior of selfassembled carbon nanotube reinforced nylon 6, 6 fibers. Compos. Sci. Technol., 70(9), 1401-1409.

[6] Gonzalez, I., Eguiazbal, J. I., Nazbal, J., 2006, Nanocomposites based on a polyamide 6-maleated styrene-butylene-co-ethylene-styrene blend: Effects of clay loading on morphology and mechanical properties. Eur. Polym. J., 42(11), 2905–2913.

[7] Tjong, S. C., Bao, S. P., 2007, Fracture toughness of high density polyethylene=SEBS-g-MA=montmorillonite nanocomposites. Compos. Sci. Technol., 67(2), 314–323.

[8] Sirong, Y., Zhongzhen, Y., Yiu-Wing, M., 2007, Effects of SEBS-g-MA on tribological behaviour of Nylon 66-organoclay nanocomposites. Tribol. Inter., 40, 855–862.

[9] Chiu, F. C., Lai, S. M., Chen, Y. L., Lee, T. H., 2005, Investigation on the polyamide 6-organoclay nanocomposites with or without a maleated polyolefin elastomer as a toughener, Polymer, 46(25), 11600–11609.

[10] Chow, W. S., Abu Bakar, A., Mohd Ishak, Z. A., Karger-Kocsis, J., Ishiaku, U. S., 2005, Effect of maleic anhydride-grafted ethylene-propylene rubber on the mechanical, rheological and morphological properties of organoclay reinforced polyamide 6-polypropylene nanocomposites. Eur. Polym. J., 41(4), 687–696.

[11] Hsieh, H. L., Quirk, R. P., 1996, Anionic Polymerization; Marcel Dekker: New York, p. 475.

[12] Cypcar, C., Camelio, P., Lazzeri, V., Mathias, L. J., 1996, Determination of chain conformation of stiff polymers by depolarized rayleigh scattering in solution. Macromolecules, 29(27), 8954-8959.

[13] Yu, J. M., Dubois, Ph., Jerome, R., 1996, Synthesis and properties of poly[isobornyl methacrylate (IBMA)-b -butadiene (BD)-b-IBMA] copolymers: New thermoplastic elastomers of a large service temperature range. Macromolecules, 29(23), 7316–7322.

[14] Jian Ming, Y. J., Philippe, D., Robert, J., 1997, Poly [glycidyl methacrylate (GMA) /methylmethacrylate (MMA)-b-butadiene (B)-b-GMA/MMA] reactive thermoplastic elastomers: synthesis and characterization. J. Polym. Sci. A: Polym. Chem., 35(16), 3507-3515.

[15] Fu, S.Y., Zheng, B., 2008, Templated silica tubes with high aspect ratios as effective fillers for enhancing the overall performance of polyimide films. Chem. Mater., 20(3), 1090-1098.

[16] Strobl, C. J., Schaflein, C., Beierlein, U., Ebbecke, J., Wixforth, A., 2004, Carbon nanotube alignment by surface acoustic waves. Appl. Phys. Lett., 85(8), 1427-1429.

[17] Zhang, F. X., Srinivasan, M. P., 2007, Multilayered gold-nanoparticle/polyimide composite thin film through layer-by-layer assembly. Langmuir, 23(20), 10102-10108.

[18] Chang, Z. J., Xu, Y., Zhao, X., Zhang, Q. H., Chen, D. J., 2009, Grafting poly(methyl methacrylate) onto polyimide nanofibers via ‘‘click’’ reaction. ACS. Appl. Mater. Interface., 1, 2804-2811.

[19] Ge, J. J., Zhang, D., Li, Q., Hou, H. Q., Graham, M. J., Dai, L. M., Harris, F.W., Cheng, S. Z. D., 2005, Multiwalled carbon nanotubeswith chemically grafted polyetherimides. J. Am. Chem. Soc., 127(28), 9984-9985.

[20] Jiang, Z. J., Huang, Z. H., Yang, P. P., Chen, J. F., Xin, Y., Xu, J. W., 2008, High PL-efficiency ZnO nanocrystallites/ PPV composite nanofibers. Compos. Sci. Technol., 68(15-16), 3240–3244.

[21] Fong, H., 2004, Electrospun nylon 6 nanofiber reinforced BIS-GMA/TEGDMA dental restorative composite resins. Polymer, 45(7), 2427-2432.

[22] Carnell, L. S., Siochi, E. J., Holloway, N. M., Stephens, R. M., Rhim, C., Niklason, L. E., Clark, R. C., 2008, Aligned mats from electrospun single fibers. Macromolecules, 41(14), 5345-5349.

[23] Tian, M., Gao, Y., Liu, Y., Liao, Y. L., Xu, R. W., Hedin, N. E., Fong H., 2007, Bis-GMA/TEGDMA dental composites reinforced with electrospun nylon 6 nanocomposite nanofibers containing highly aligned fibrillar silicate single

crystals. Polymer, 48(9), 2720-2728.

[24] Hussain, S. T., Mazhar, M., Gul, S., Khan, M. A., 2009, Novel catalyst to manufacture carbon nanotubes and hydrogen gas. U.S. 2009208403, Aug. 20.

[25] Kausar, A., Hussain, S. T., 2013, Effect of multi-walled carbon nanotubes reinforcement on the physical properties of poly(thiourea-azo-ether)-based nanocomposites. J. Plast. Film. Sheet. DOI: 10.1177/8756087913487003.

[26] King, J. A., Klimek, D. R., Miskioglu, I., Odegard, G. M., 2013, Mechanical properties of graphene nanoplatelets/epoxy composites. J. Appl. Polym. Sci., 128(6): 4217–4223.

[27] Dassios, K. G., Musso, S., Galiotis, C., 2012, Compressive behaviour of MWCNT/epoxy composite mats. Compos. Sci. Technol., 72(9): 1027–1033.

[28] Kausar, A., Hussain, S. T., 2013, Elastomeric blends of poly(styrene-butadiene-styrene) and conductive heteroaromatic poly(thiourea-azo-ether): Tensile and thermal properties. J. Elast. Plast., DOI: 10.1177/0095244313489909.

[29] Deitzel, J. M., Kosik, W., McKnight, S. H., Ten, N. C. B., Desimone, J. M., Crette, S., 2002, Electrospinning of polymer nanofibers with specific surface chemistry. Polymer, 43(3), 1025–1029.

[30] Demczyk, B.G., Wang, Y. M., Cumings, J., Hetman, M., Han, W., Zettl, A., Ritchie, R. O., 2002, Direct mechanical measurement of the tensile strength and elastic modulus of multiwalled carbon nanotubes. Mater. Sci. Eng. A., 334(1-2), 173–178.

[31] Ding, B., Kim, H. -Y., Lee, S. -C., Shao, C. -L., Lee, D. -R., Park, S. -J., Kwag, G. -B. and Choi, K. J., 2002, Preparation and Characterization of a nanoscale poly(vinyl alcohol) fiber aggregate produced by an electrospining method. J. Polym. Sci. B: Polym. Phy., 40(13), 1261–1268.